Creep-Fatigue in Biaxial Stress States using Cruciform Specimen

Masao Sakane and Masateru Ohnami

Faculty of Science and Engineering, Ritsumeikan University, Kyoto, Japan

Third International Conference on Biaxial/Multiaxial Fatigue,

April 3-6, 1989, Stuttgart FRG

1.Introduction

Most of structural components suffer more or less multiaxial damage rather than uniaxial damage, but multiaxial low cycle study from a viewpoint of developing an appropriate design criterion is a few because of the cost and difficulty of experiments[1-3]. Historically, there have been proposed many multiaxial fatigue criteria which were extensively reviewed by Garud[4] but there is no systematic research by applying these criteria to the experimental data in order to find out a proper criterion.

On a criterion used in the practical design of the structural components which receive multiaxial damage, we have to confirm the safety of the criterion by applying it to the low cycle fatigue data obtained in widely ranged multiaxial stress states. Combined push-pull/reversed torsion fatigue tests have been frequently made but this type of test cannot achieve a wide range of multiaxial stress states. The principal strain ratio which can be covered in the test is between -1 and -0.5, where the principal strain ratio is the ratio of the minimum principal strain to the maximum principal strain. Multiaxial fatigue test, which can cover a more widely ranged principal strain ratio, is needed.

This paper describes a new multiaxial low cycle machine for a cruciform specimen, and also describes the test results in high temperature multiaxial low cycle fatigue carried out in the principal strain ratio

between -1 and 1. The material tested was 1Cr-1Mo-1/4V and type 304 austenitic stainless steels. The discussion was made on the effect of stress multiaxiality on low cycle fatigue life and crack mode.

2.Cruciform Specimen.

The shape of the cruciform specimen was determined from the FEM analysis so that the stress and strain distribute uniformly along the gage length. The shape of the specimen and the finite element mesh are shown in Figs. 1 and 2. The coordinate system used in this paper is also shown in Fig.1. The FEM analysis was made for a quarter part of the specimen considering the symmetry of the stress and strain. The thickness of the mesh excluding part A is 12 mm and that of part A is gradually reduced from 6 mm to 1 mm. The thickness of the gage length is 1 mm. An isotropic 8-node element with 3x3 Gaussian points was used. Number of elements and nodes are respectively 159 and 530. The computer program ADINA was used in the analysis.

Figure 3 shows the cyclic constitutive stress-strain relation in the incremental/decremental test[5] at the Mises' strain rate of 0.1%/sec. The test was carried out in the push-pull and reversed torsion. The cyclic stress-strain relation is well correlated with the Mises' parameter[5]. The material constants used to the FEM analysis was ; Young's modulus was 2 05 GPa and yield stress was 410 MPa. The stress-strain relation post yield was approximated by 7 lines.

Figure 4 shows an example of the stress and strain distribution along the gage length for 1Cr-1Mo-1/4V steel in biaxial tension, i.e., in the ϕ=1 test. In this paper, the principal strain ratio (ϕ) is defined as the ratio of the minimum principal strain to the maximum principal strain on the specimen surface, that is, ϕ is defined as $\phi = \varepsilon_x / \varepsilon_y$ in the

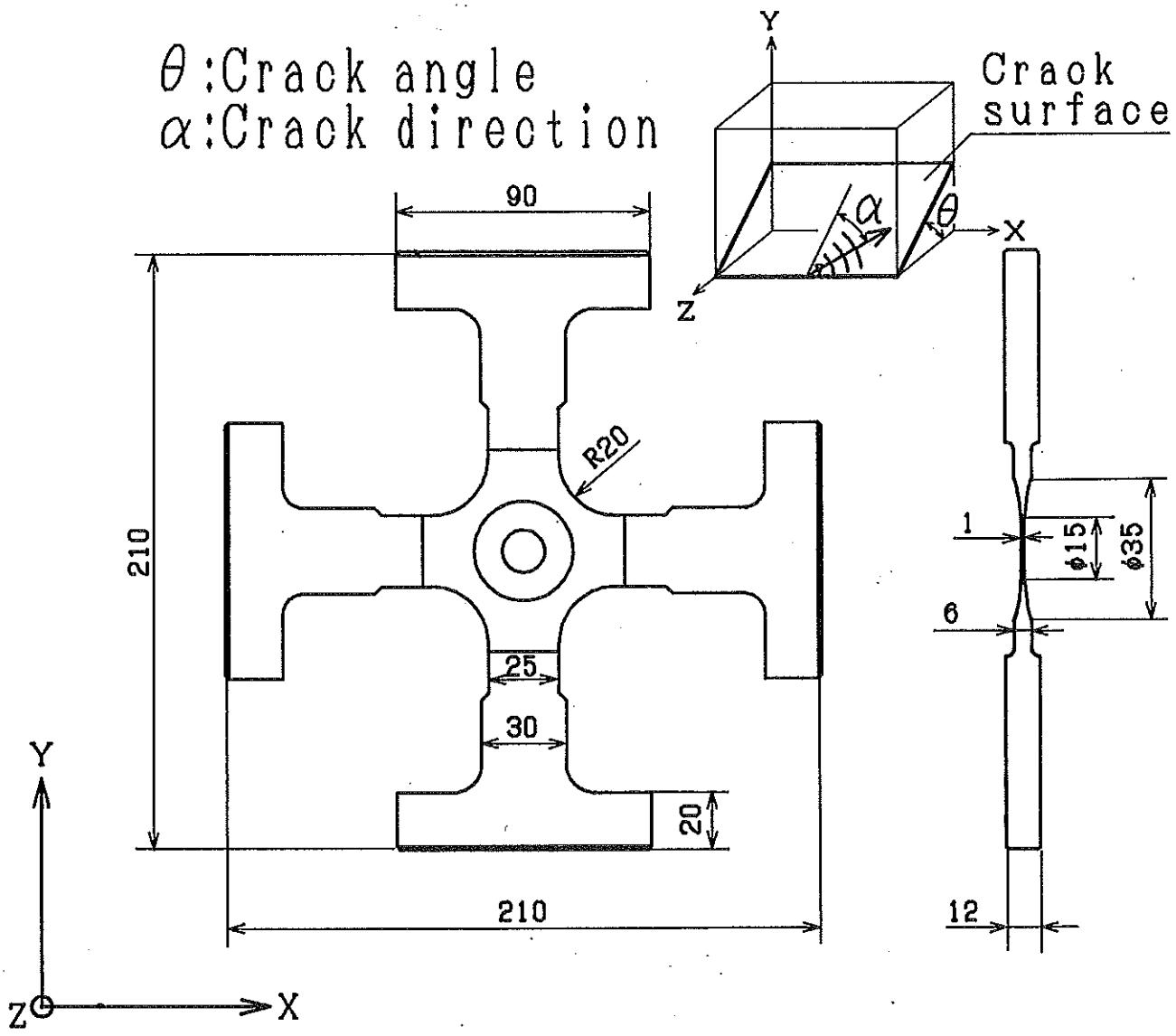

Fig.1 Shape and dimensions of the cruciform specimen together with the coordinate system.

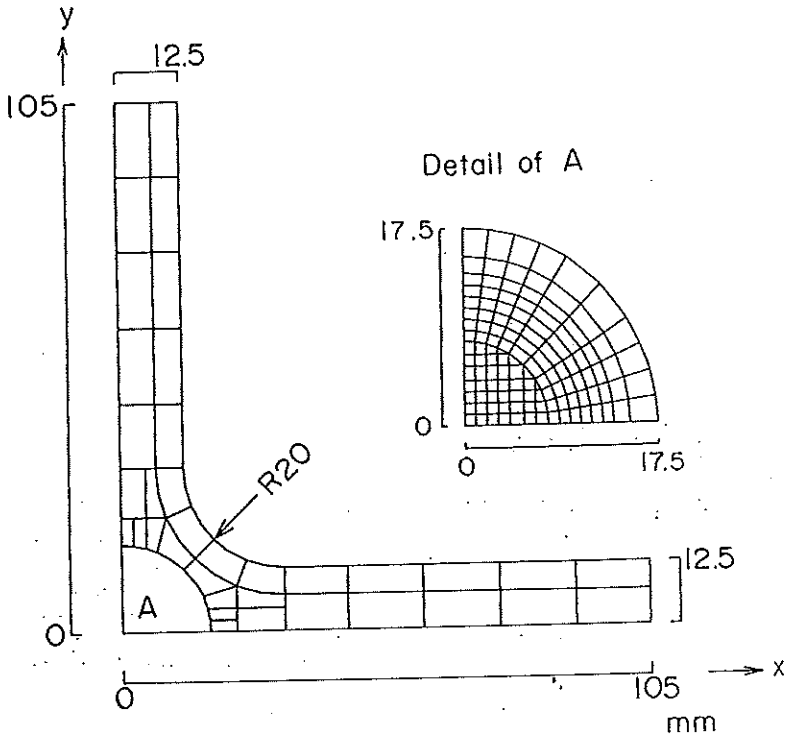

Fig.2 FEM mesh for the stress and strain analysis.

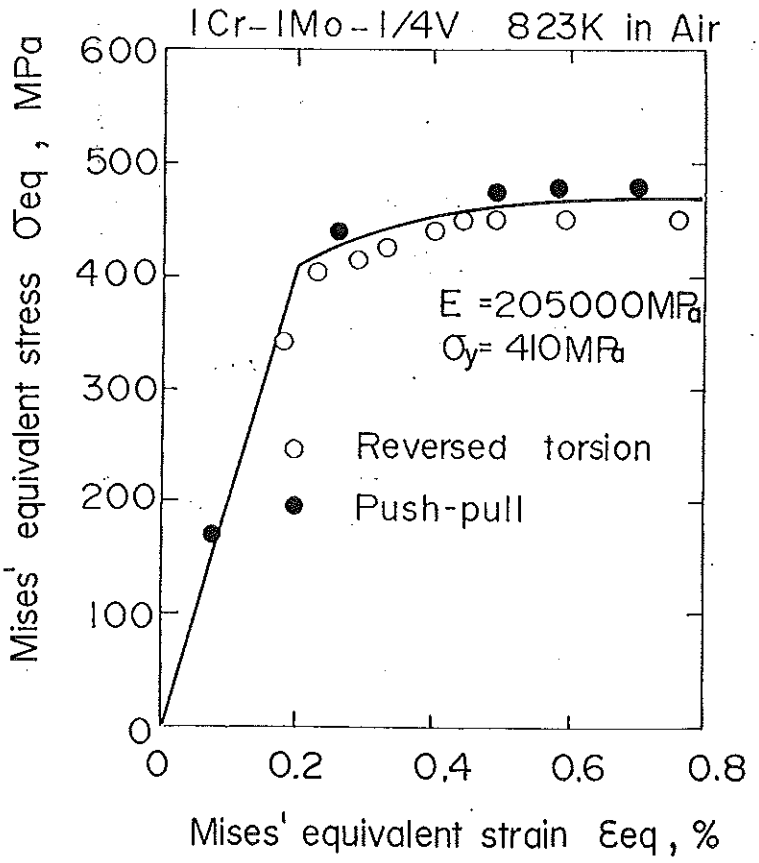

Fig.3 Cyclic constitutive relation of 1Cr-1Mo-1/4V steel in the incremental/decremental test at 823 K.

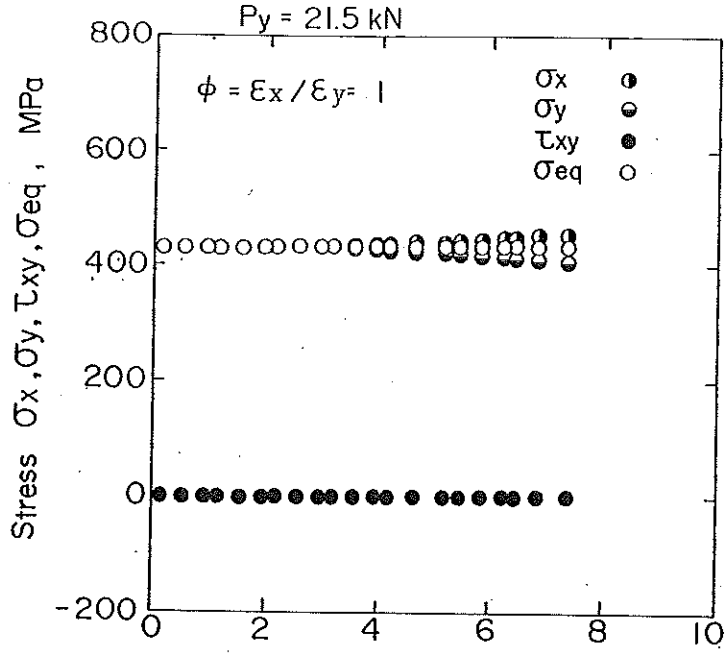

(a) Stress distribution.

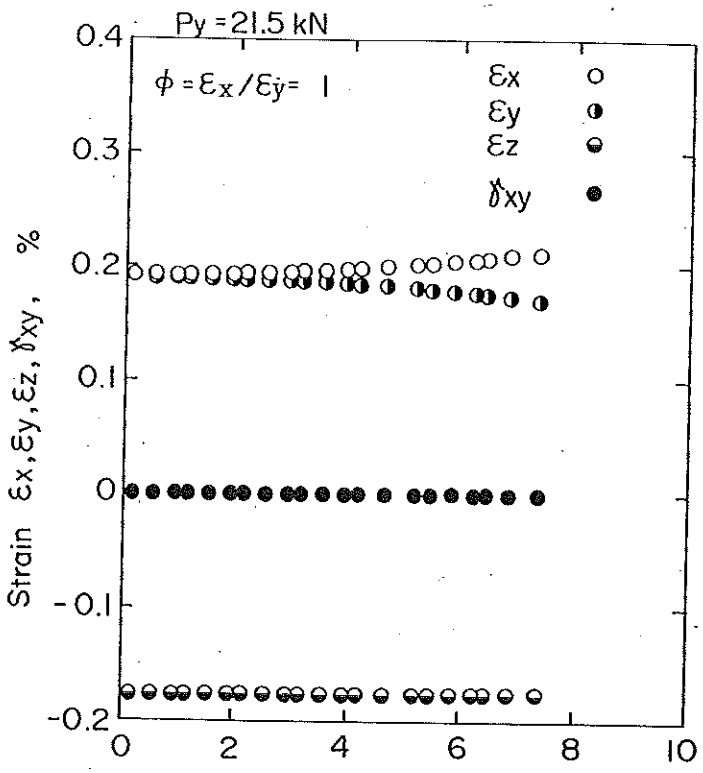

(b) Strain distribution.

Fig.4 Stress and strain distribution along the gage length in the ϕ =1 test for 1Cr-1Mo-1/V steel.

coordinate system in Fig.1. Figure 4 clearly shows that the variation of the stress and strain is very small up to the 5-mm gage length, so the authors judged that the specimen geometry shown in Fig.1 is suitable for the biaxial low cycle fatigue test.

The specimen used in the study requires the extensometry in two directions, x and y. The displacement along the gage length was measured by an originally designed extensometer which can measure the displacement in two directions without interfering each other. The extensometer was pressed by springs to the specimen through a window of the electric resistance furnace. The crack of the notched specimen was monitored with a microscope through the other window. The power of the furnace was 3 KW. The temperature variation along the gage length was within 5 K.

3. Biaxial Low Cycle Fatigue Apparatus.

The experimental apparatus used in the study is an originally designed electric-hydraulic servo machine for the cruciform specimen. Figures 5 and 6 show the general view and control flow of the apparatus. The apparatus has four actuators and four servo controllers to generate a wide range of biaxial stress states. When conducting strain controlled experiments using this type of the apparatus, the control which gives no movement of the specimen center is essential. If we employ the conventional control, where the servo system takes the feedback signal from the extensometer, the unmovement of the specimen center may not be guaranteed. The reason is that the small unbalanced control in a direction, x or y, will disturb the control of the other direction. The system does not reach the stable state.

In order to achieve the control with no movement of the specimen center, the apparatus basically controls the stroke of the actuators. In

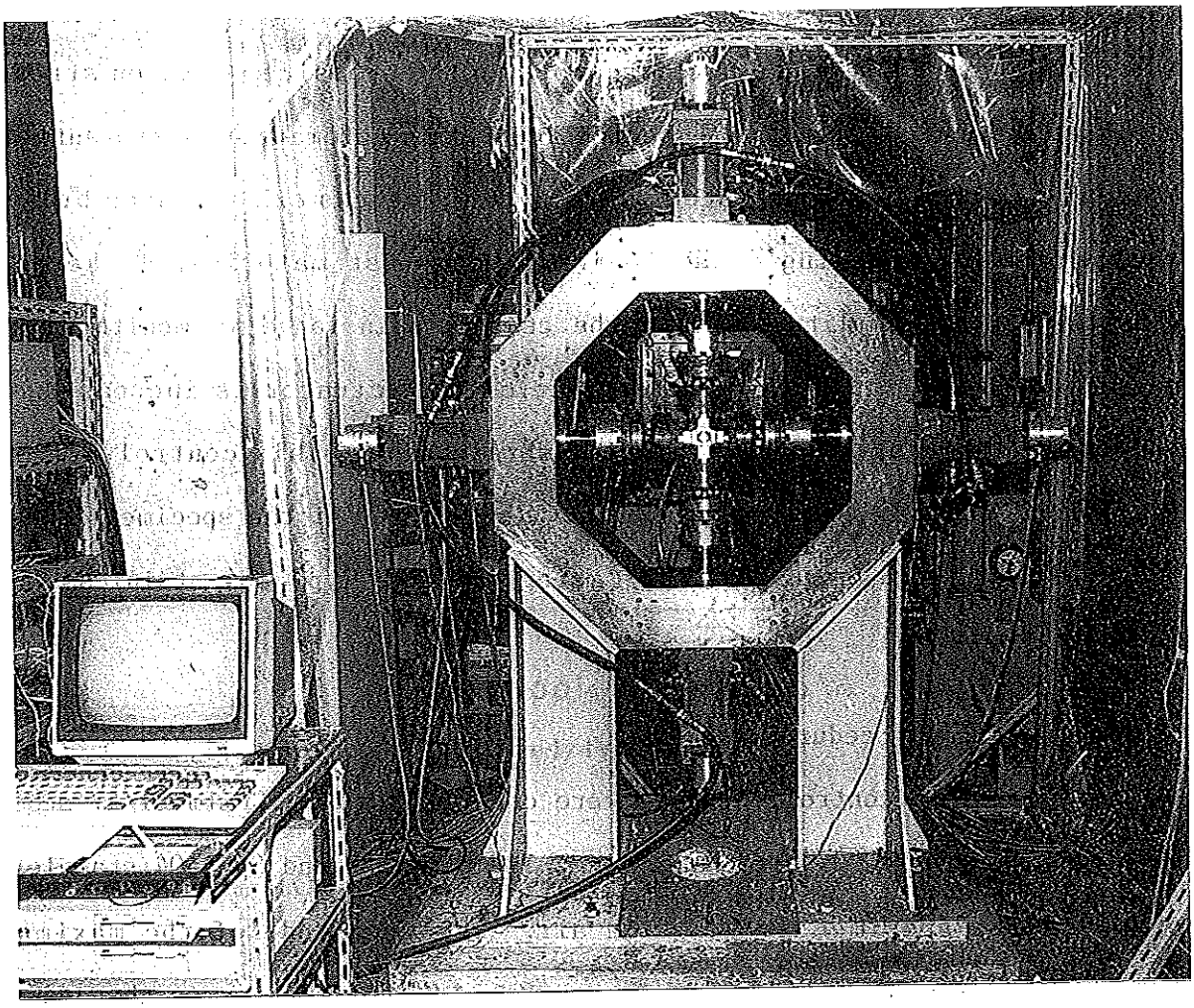

Fig.5 General view of the test apparatus.

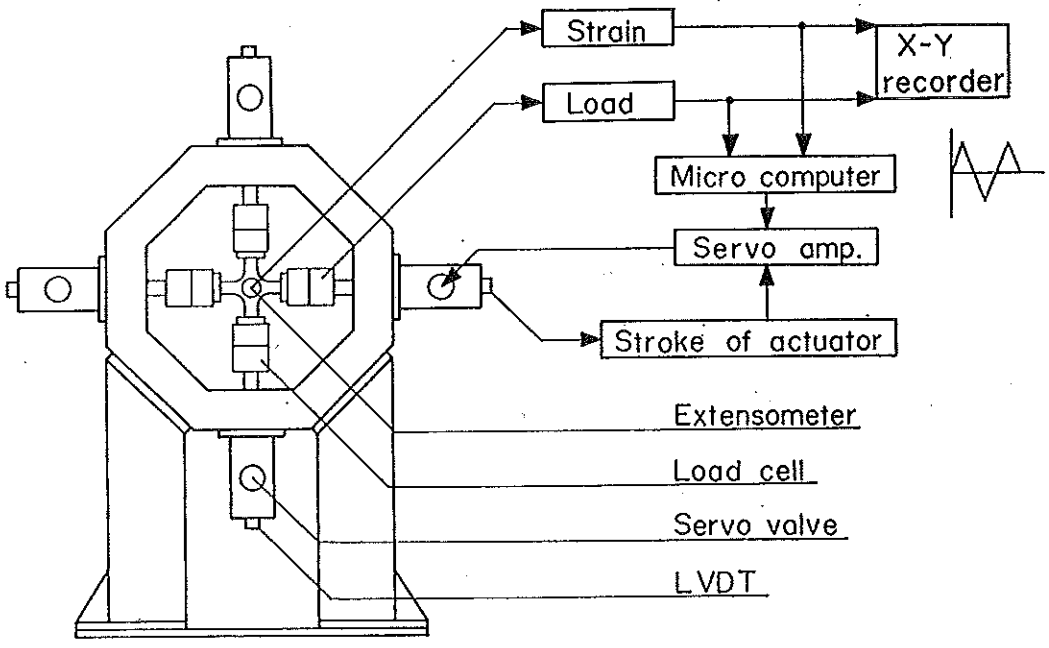

Fig.6 Control flow of the test apparatus.

the stroke control, if the two actuators in the opposite position stroke equally, the unmovement of the specimen center is automatically guaranteed. However, in that control system, strain will reduces or increases by the cyclic strain hardening or softening of the test material. To keep a constrain strain amplitude during the test, strain range is monitored at each cycle by a computer and the stroke of the actuator is increased or decreased in order to give a testing strain range. This control system enabled the accurate experiment without the movement of the specimen center for cyclic hardening and softening materials like type 304 stainless and Cr-Mo-V steels.

4. Experimental Procedure.

Total strain controlled tests were carried out for 1Cr-1Mo-1/4V steel specimen which has a 0.5-mm center notch hole at 823K and SUS 304 stainless steel smooth specimen at 923 K in air. The amplitude of the maximum principal strain was fixed and the minimum principal strain was changed to achieve the different principal strain ratio ranging from -1 to 1. The heat treatment of 1Cr-1Mo-1/4V steel was that; 5hr at 923K, 19hr at 1288 K, fan cooled, 38hr at 953 K and furnace cooled. SUS 304 stainless steel received a solution treatment at 1373 K. The maximum principal strain rate was 0.1 %/sec. The failure cycle in the paper was defined as the cycle at which the tensile stress amplitude normal to the crack decreases to 3/4 of the maximum value.

5. Experimental Results and Discussion.

5.1 Biaxial Low Cycle Fatigue Life.

Figures 7 (a) and (b) respectively show the fatigue life of 1Cr-1Mo-1/4V and SUS 304 stainless steels. The maximum principal strain range is

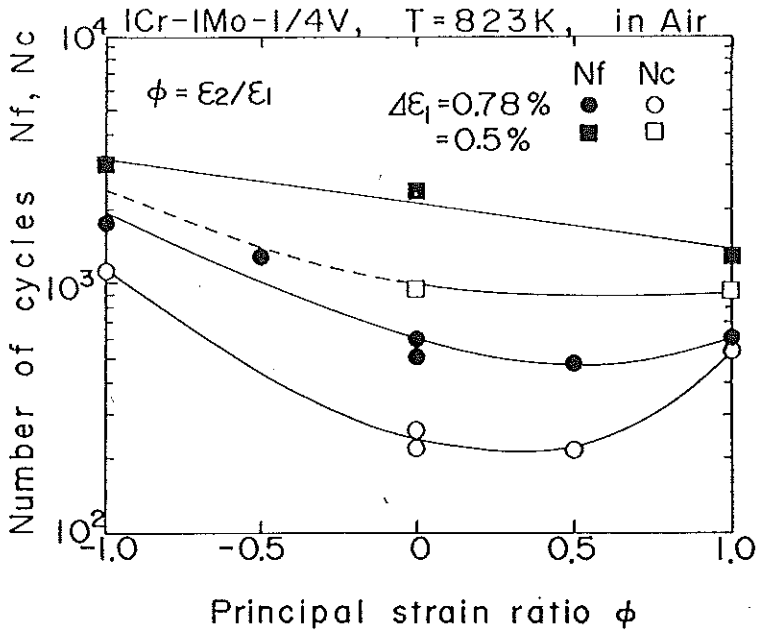

(a) 1Cr-1Mo-1/4V steel at 823 K.

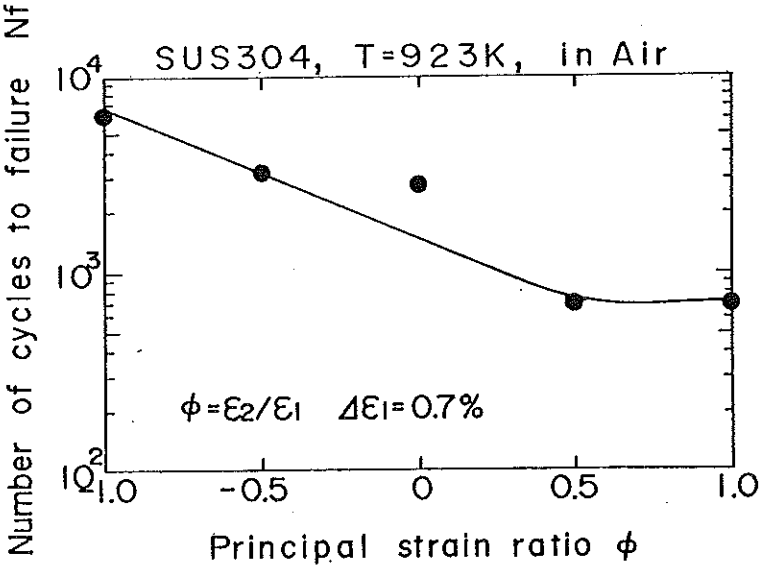

(b) SUS304 steel at 923 K.

Fig.7 Variation of failure cycle with the principal strain ratio for (a) 1Cr-1Mo-1/4V steel and (b) SUS 304 steel.

0.78 % and 0.5 % for 1Cr-1Mo-1/4V steel, and is 0.7 % for SUS 304 steel. The crack initiation cycle was defined as the cycle of 0.1 mm crack extension from the notch hole observed by a microscope. The figures clearly show that the strain biaxiality affects the low cycle fatigue life. In the fixed maximum principal strain test, the fatigue life decreases with increasing the principal strain ratio. The minimum fatigue life takes place in the principal strain ratio between 0.5 and 1.

The crack initiation life, defined as the 0.1 mm crack extension, has almost the same dependency as the failure life, and the ratio of the crack initiation life to the failure life was 0.5 except the ϕ =1 test. The crack initiation life in that test, i.e., in the equi-biaxial tension/compression test, the ratio is larger than that in the other test and is 0.9. This is attributed to the fact that, in that test, the applied load was much larger than that in the other tests and the material was very damaged by the larger applied stress. Since the crack propagated through the damaged material, which presumably results in the larger crack propagation rate.

Conventional biaxial low cycle tests have been commonly carried out in the combined push-pull and reversed torsion. The principal strain ratio achieved by this test is between -1 and -0.5. The test results in Figs.7 (a) and (b) showed that the biaxial low cycle fatigue life decreased with increasing ϕ in the maximum principal strain controlled test. The minimum fatigue life yields in the principal strain ration between 0.5 and 1. So, we have to confirm the safety of the multiaxial low cycle fatigue criterion by applying it to the multiaxial low cycle fatigue data in the wide range of the principal strain ratio.

The authors have extensively discussed the applicability of the multiaxial low cycle fatigue criterion in the previous paper[6], where six

strain and four stress criteria were examined. The experimental data fitted to the criteria were obtained in the combined push-pull and reversed torsion. The COD strain [7-9] and Γ-plane parameter[10,11] were effective as a strain criterion and only the COD stress[7-9] was effective as a stress criterion. The discussion on the applicability of multiaxial stress/strain criteria is presented in this conference by the authors[12], so the discussion on it is not presented here to avoid the repetition. The only point the authors wish to state is that the COD stress and strain can correlate well the biaxial low cycle fatigue life in the test with the principal strain ratio between -1 and 1.

5.2 Crack Mode in Biaxial Low Cycle Fatigue.

The crack propagation direction was extensively observed on the specimen after the test. Figure 8 shows the crack propagation direction on the specimen surface for 1Cr-1Mo-1/4V and SUS 304 steels. The crack appears to propagate in mode I in all the tests except the SUS 304 smooth specimen at ϕ =-1. In that test, small zig-zag cracks, which were mode II, linked up to propagate in mode I.

The crack mode cannot be completely determined without defining the propagation direction into the specimen. In order to determine the crack mode taking account of the propagation direction into the specimen, the extensive observation was made. Figure 1 showed the definition of the crack angles θ and crack direction α on the fracture surface, where θ is the angle of the crack surface against y-plane and α the angle from x-plane.

Figure 9 shows the variation of θ and α with the propagation of cracks in the ϕ =0 test for (a) 1Cr-1Mo-1/4V and (b) SUS 304 steels. The crack initiates at the notch edges for 1Cr-1Mo-1/V steel and at the point

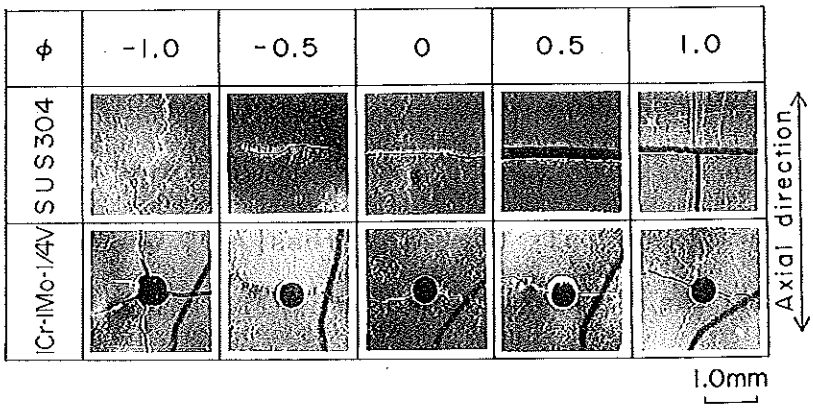

Fig.8 Crack propagation direction on the specimen surface.

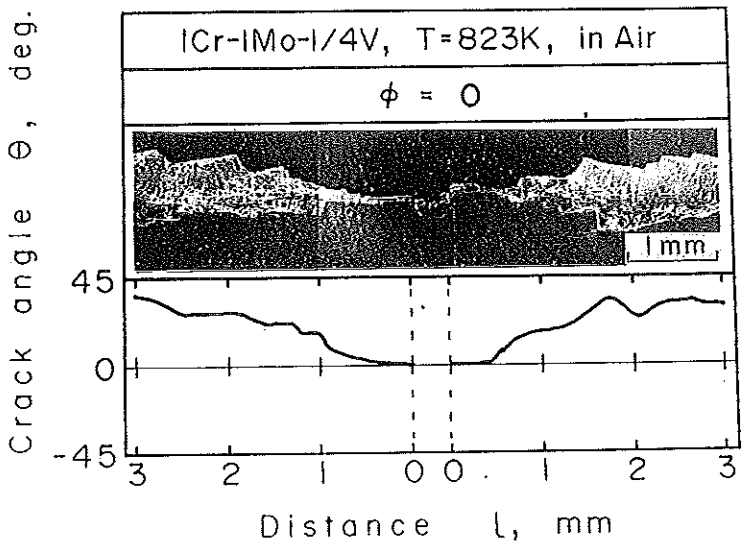

(a) 1Cr-1Mo-1/4V steel.

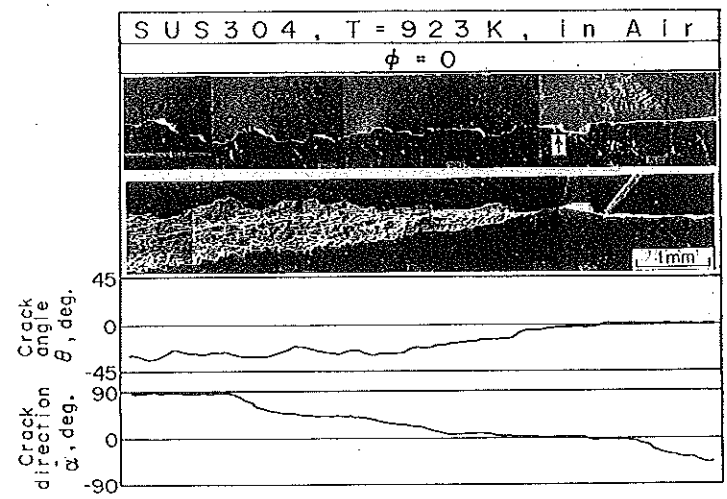

(b) SUS 304 stainless steel.

Fig.9 Variation of the crack angle θ and crack direction α in the ϕ=0 test for (a) 1Cr-1Mo-1/4V steel and (b) SUS 304 steel.

where an arrow indicates for SUS 304 steel. The crack initiation point was confirmed by the observation of the striation direction. For both the steels, the crack initiates on the $\theta=0$ plane in the $\alpha=0$ direction, which means that the crack initiates on the normal plane to the free surface and propagates in z-direction. The crack initiated on that plane propagates in the direction of increasing/decreasing α. At the same time, the crack plane begins to incline in the direction of increasing/decreasing θ. The final crack propagation is in the direction of $\alpha=90$ degree on the $\theta=45$ degree plane, of which propagation behavior appears to be stable.

Figure 10 summarizes the plane where the crack propagated. The broad line indicates the maximum shear stress plane or the maximum principal stress plane. The dashed plane is the plane on which we could find the crack. Also Table 1 lists the plane on which the crack propagated. In the table, ε_1 indicates the maximum principal plane, and ε_2 and $_3$ are respectively the second and third principal planes. The symbol $\varepsilon_{1,2}$ shows that the crack was found on both the second and third principal planes. γ_{max} indicates the maximum shear plane. The single asterisk indicates that the crack was partly found on that plane and double asterisks means that the crack was confirmed near the notch. The similar classification of cracks at room temperature was made by Brown and Miller[13].

The summary of the crack plane is :

(1)In the $\phi=-1$ test which corresponds to the reversed torsion test using hollow cylindrical specimens, we confirmed both the mode I and II cracks. The crack tends to propagate in mode I as the crack length increases.

(2)In the test with the principal strain ratio between -0.5 and 0.5, the crack nucleates in mode I and changes the propagation plane to the maximum shear stress plane as the crack length increases, which is typically found

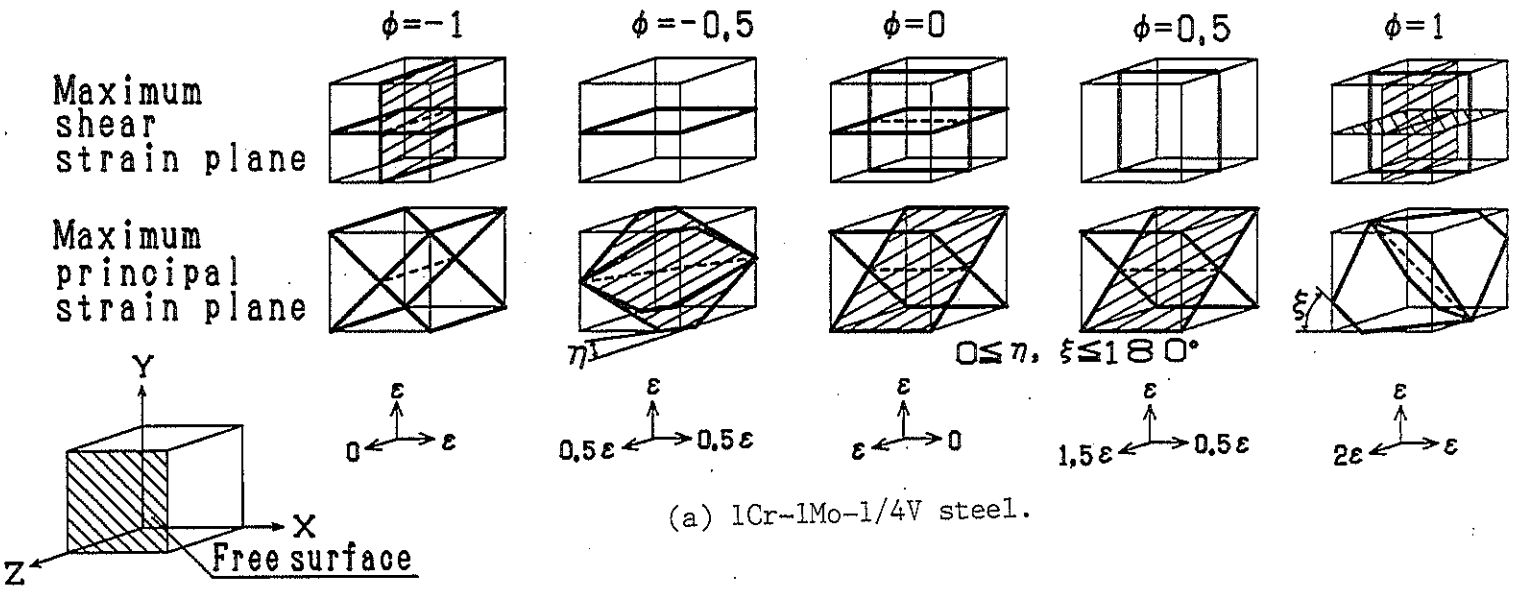

(a) 1Cr-1Mo-1/4V steel.

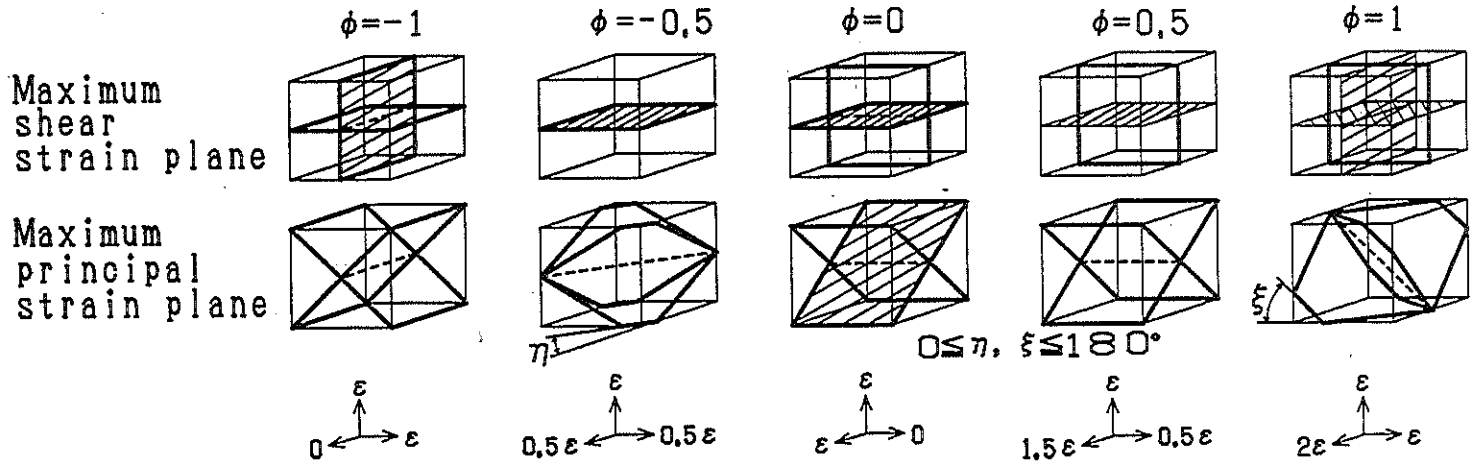

(b) SUS 304 stainless steel.

Fig.10 The plane on which the crack propagated. The broad line shows the maximum shear strain or maximum principal strain planes. The shaded plane was the plane of the crack propagation.

in the 1Cr-1Mo-1/4V notched specimen. On the SUS 304 smooth specimen, the crack nucleates at many places so that the linking may occur before the complete change in the propagation plane. However, the inclination is observed as shown typically in the $\phi=0$ test.

(3)In the $\phi=1$ test, the crack nucleates and propagates on the second and third principal planes.

Above consideration shows that, in the test with the principal strain ratio between -0.5 and 0.5, the crack nucleates normal to the maximum principal stress plane and tends to propagate on the maximum shear stress plane for both the notched and smooth specimens. The crack in this principal strain range can be regarded as a stable crack propagation in the sense that the crack does not coexist on the different planes. On the other hand, the crack in the $\phi=-1$ test, the crack was found on both the maximum principal stress and shear stress planes. The crack propagation appears to be unstable in this test since the crack sometimes propagates on the different plane depending on the testing condition.

The authors[6,14] have found, in the reversed torsion test, using the SUS 304 hollow cylindrical specimen which is the same testing condition as $\phi=-1$ test in this paper, that the crack propagated in mode II in the smooth specimen but in mode I in the notched and precracked specimens. The direction of the precrack had no effect on the post crack extension. In the smooth specimen, the microcrack was mode I but semimicro and macrocrack were mode II. Thus, in this type of test, the specimen only fails by mode II macro crack only when the linking process of many mode II semimicro crack is the major fracture process[6]. If a few major crack propagate stably, the crack always mode I in the $\phi=-1$ test[6,14].

In the $\phi=1$ test, i.e., the equi-biaxial tension/compression test, the specimen fails by the crack on the second and third maximum principal

Table 1 Summary of the crack plane.

ϕ	-1	-0.5	0	0.5	1
1Cr-1Mo-$\frac{1}{4}$V	$\varepsilon_{1,2}^{**}$ γ_{max}^{**} $\rightarrow \varepsilon_{1,2}$	$\varepsilon_{1,2}^{**} \rightarrow \varepsilon_1^{*}$ γ_{max}	$\varepsilon_{1,2}^{**} \rightarrow \gamma_{max}$	$\varepsilon_2^{**} \rightarrow \gamma_{max}$	$\varepsilon_{2,3} \rightarrow \varepsilon_{2,3}$ γ_{max}^{*}
SUS304	$\varepsilon_{1,2}$ γ_{max}	ε_1 γ_{max}^{*}	$\varepsilon_{1,2} \rightarrow \gamma_{max}$	ε_2 γ_{max}^{*}	$\varepsilon_{2,3}$

* partly observed crack
** crack near the notch (smaller than 0.1mm in length)

strain plane. Normal strain on z-plane, i.e., the strain on the plane parallel to the free surface has the maximum amplitude but there works no normal stress on that plane so that the crack does not nucleate and does not propagate. Therefore, only the strain amplitude is not sufficient parameter as a biaxial low cycle fracture criterion but also we have to take account of the stress component.

6. Conclusions.

(1)High temperature biaxial low cycle fatigue machine, which can perform the experiments with the principal stress ratio between -1 and 1, was developed.

(2)In the maximum principal strain controlled test, the biaxial low cycle fatigue life reduced with increasing the maximum principal strain ratio. The minimum life was observed in the principal strain ratio between 0.5 and 1 for 1Cr-1Mo-1/4V and SUS 304 steels.

(3)The crack initiated in mode I in the principal strain ration between -0.5 and 0.5 and changed the direction to the maximum shear strain plane. The crack on both the maximum principal and shear strain plane was found in the ϕ=-1 test. In the ϕ=1 test, the crack nucleated and propagated on the second and third principal strain planes.

Acknowledgment

The authors wish to express gratitude to Mr. T. Ito, the research assistant Ritsumeikan University, for carrying out the biaxial fatigue test and observation of the fracture surface.

References

[1] Krempl, E., "The Influence of State of Stress on Low-Cycle Fatigue of Structural Materials - A Literature Survey and report," ASTM STP, No.549, 1974.

[2] Brown, M. W., and Miller, K. J., "Two Decades of Progress in the Assessment of Multiaxial Low Cycle Fatigue Life," ASTM STP, No.770, 1982, pp.482-499.

[3] Ohnami, M., Sakane, M., and Hamada, N., "A Review on Biaxial Low-Cycle Fatigue in Creep Region at Elevated Temperatures," J. Soc. Mater. Sci., Japan, Vol.35, 1986, pp.230-240.

[4] Garud, H. S., "Multiaxial Fatigue : A Study of the State of the Art," J. Testing and Evaluation, Vol.9, 1981, pp.165-178.

[5] Ohnami, M., Sakane, M., and Nishino, S., "Cyclic Behavior of a Type 304 Stainless Steel in Biaxial Stress Stated at Elevated Temperatures," Inter. J. Plasticity, Vol.4, pp.77-89.

[6] Sakane, M., Ohnami, M., and Sawada, M., "Fracture Modes and Low Cycle Biaxial Fatigue Life at Elevated Temperature," J. Eng. Mater. Tech., Trans. ASME, Vol.109, 1987, pp.236-243.

[7] Hamada, N., Sakane, M., and Ohnami, M., "Creep-Fatigue Studies Under a Biaxial Stress State at Elevated Temperature," Fatigue Eng. Mater. Struct., Vol.7, 1984, pp.85-96.

[8] Hamada, N., Sakane, M., and Ohnami, M., "A Study of High Temperature Low Cycle Fatigue Criterion in Biaxial Stress State," Bull. Japan Soc.

Mech. Eng., Vol.28, 1985, pp.1341-1347.

[9] Hamada, N., Sakane, M., and Ohnami. M., "Effect of Temperature on Biaxial Low Cycle Fatigue Crack Propagation and Failure Life of an Austenitic Stainless Steel," Proc. 30th Japan Congr. Mater. Res., 1987, pp.69-75.

[10] Kandil, F. A., Brown, M. W., and Miller, K. J., "Biaxial Low-Cycle Fatigue Failure of 316 Stainless Steel at Elevated Temperatures," Mech. Behav. Nucl. Appl. Stainless Steel Elevated Temperature, 1982, pp.203-209.

[11] Lohr, R. D., and Ellison, E. G., "A Simple Theory for Low Cycle Multiaxial Fatigue," Fatigue Eng. Mater. Struct., Vol.3, 1980, pp.1-17.

[12] Hamada, N., Sakane, M., and Ohnami, M., "COD Criterion to Assess High Temperature Biaxial Low Cycle Fatigue," 3rd Inter. Conf. Biaxial/Multiaxial Fatigue, 1989, Stuttgart.

[13] Brown, M. W., and Miller, K. J., "Initiation and Growth of Cracks in Biaxial Fatigue," Fatigue Eng. Mater. Struct., Vol.1, 1979, pp.231-246.

[14] Sakane, M., Ohnami, M., and Hamada, N., "Biaxial Low Cycle Fatigue for Notched, Cracked and Smooth Specimens at High Temperature," J. Eng. Mater. Tech., Trans. ASME, Vol.110, 1988, pp.48-54.